

# Scaling properties and classification of Single Step growth model in (2+1)-dimensions

H. Dashti-Naserabadi,<sup>1,\*</sup> A. A. Saberi,<sup>2,†</sup> and S. Rouhani<sup>1,‡</sup>

<sup>1</sup>*Department of Physics, Sharif University of Technology, Tehran 11155-9161, Iran*

<sup>2</sup>*Department of Physics, University of Tehran, Tehran 14395-547, Iran*

(Dated: March 5, 2013)

## Abstract

We study the (2+1)-dimensional single-step model (SSM) with a tunable parameter  $p$ . Using extensive numerical simulations, we find dependence of interface exponents and scaling exponents derived from iso-height clusters on  $p$ . Also we test the iso-height contours for being Schramm-Loewner evolution (SLE $_{\kappa}$ ) curves. We find that there is convincing evidence that they are with  $k \approx 8/3$  at  $p = 0$ , but for  $p \neq 0$ , the results do not match with each other. Furthermore, the boundary conditions become important for  $p \neq 0$ . The right choice of boundary conditions at  $p = 0.5$  such that Gaussian free field universality class emerges, remaining unknown.

## I. INTRODUCTION

Growth processes and rough surfaces are interesting topics in physics from both theoretical and experimental points of view [1, 2]. Various discrete models have been suggested to describe surface growth processes, for examples see [1, 2]. These models produce a self-affine interface  $h(\mathbf{x})$  such that its probability distribution function remains invariant under scale transformation:

$$h(\mathbf{x}) \cong b^{-\alpha} h(b\mathbf{x}), \quad (1)$$

where  $\cong$  means statistically the same, and  $\alpha \geq 0$ . A possible way for classification of various surface growth models is based on scaling behaviour of surface width,  $w(t, L) = \sqrt{\langle [h(\mathbf{x}, t) - \langle h \rangle]^2 \rangle}$ , and  $\langle \cdot \rangle$  denotes spacial averaging. For a non-equilibrium growth, the width is expected to have the following scaling form [3]

$$w^2(t, L) \sim L^{2\alpha} f\left(\frac{t}{L^z}\right). \quad (2)$$

The scaling function  $f$  usually has the asymptotic form  $f(x \rightarrow \infty) = \text{constant}$  and  $f(x \rightarrow 0) \sim x^{2\beta}$ . The saturation time  $t_s$  has the scaling ansatz  $t_s \sim L^z$ . The universality class can then be given by two independent roughness and growth exponents,  $\alpha$  and  $\beta$ , respectively.

---

\* h\_dashti@physics.sharif.edu

† ab.saberi@ut.ac.ir

‡ srouhani@sharif.ir

The dynamic exponent is  $z = \alpha/\beta$ .

For some equilibrium-rough interfaces, the width behaves logarithmically [4], i.e.,  $w^2(t, L) \sim \ln t$  for  $t \ll t_{sat}$ , and  $w^2(t, L) \sim \ln L$  for  $t \gg t_s$ , with  $z = 2$ .

Whether rough surfaces fall into discrete universality classes is unknown, however many self-affine surfaces are observed to belong to certain universality classes. Two well known universality classes are described by continuous Langevin equations i.e., the Edwards-Wilkinson (EW) [4] and the Kardar-Parisi-Zhang (KPZ) [5] equations. The KPZ equation is given by

$$\frac{\partial h(\mathbf{x}, t)}{\partial t} = \nu \nabla^2 h + \frac{\lambda}{2} |\nabla h|^2 + \eta(\mathbf{x}, t), \quad (3)$$

where the relaxation term is caused by a surface tension  $\nu$ , and the nonlinear term is due to the lateral growth. The noise  $\eta$  is uncorrelated Gaussian white noise in both space and time with zero average i.e.,  $\langle \eta(\mathbf{x}, t) \rangle = 0$  and  $\langle \eta(\mathbf{x}, t) \eta(\mathbf{x}', t') \rangle = 2D \delta^d(\mathbf{x} - \mathbf{x}') \delta(t - t')$ . For  $\lambda = 0$ , the EW equation is retrieved whose exact solution  $\alpha = (2 - d)/2$  and  $z = 2$ , is known in  $(d + 1)$ -dimensions [4]. For KPZ equation, due to additional scaling relation  $\alpha + z = 2$ , there remains only one independent exponent, say  $\alpha$ . The exact solution only exists in  $1d$  [5] which gives  $\alpha = 1/3$ . In  $2d$ , the exponent is available only by various simulations and theoretical approximations ranging from  $\alpha = 0.37$  to  $0.4$  [6–8].

A new tool for study of domain walls in critical systems is the theory of Schramm-Loewner Evolution (SLE) [9]; for a review see [10]. The scaling behaviour of the two-dimensional critical lattice models can be reflected in the statistics of non-crossing random curves which form the boundaries of clusters on the lattice.

In the 1920s, Loewner studied simple curves growing from the origin into the upper half-plane  $\mathbb{H}$  [11]. Loewner's idea was to describe the evolution of these curves in terms of the evolution of the analytic function  $g_t(z)$ , which conformally maps the region  $\mathbb{H} \setminus K_t$  to  $\mathbb{H}$ , where  $K_t$  is the hull (the union of the curve and the set of points which can not be reached from infinity without intersecting the curve). He showed that this function satisfies the following differential equation:

$$\frac{dg_t}{dt} = \frac{2}{g_t(z) - \xi_t}, \quad (4)$$

for a real continuous function  $\xi_t$ , related to the image of the tip of the curve under  $g_t$ .

More recently, Schramm proposed the idea that a measure on the continuous driving functions  $\xi_t$  would induce a measure on the set of growing curves in  $\mathbb{H}$ , and showed that the latter measure is conformally invariant if and only if  $\xi_t = \sqrt{\kappa} B_t$ . The diffusivity constant  $\kappa$  determines the critical exponents, hence, the universality class of the system in question. Some authors have argued that

$\text{SLE}_\kappa$  may be applied to surface growth phenomena as well[12–15].

In this paper we study  $2d$  single step model (SSM) [16–19], a kind of solid on solid (SOS) model [20] which is defined as follows. One column  $(i, j)$  is chosen randomly, if it is a local minimum then its height is increased by 2 with probability  $p_+$ ; one can consider this process as deposition. If it is a local maximum then its height is decreased by 2 with probability  $p_-$ , as a process of desorption or evaporation. This definition guarantees that in each step, the height difference between two neighboring sites is exactly one. Overhanging is not allowed in this model and the interface will not develop large slopes. We start with the initial condition  $h(i, j; t = 0) = [1 + (-1)^{i+j}]/2$  where  $1 \leq i \leq L_x$  and  $1 \leq j \leq L_y$ . We impose the condition  $p_+ + p_- = 1$ , so due to up/down symmetry  $p_+ \leftrightarrow (1 - p_+)$ , we just need to consider  $p_+ \leq 0.5$ . Here after we shall refer to  $p_+$  as  $p$ .

Several papers have investigated this model, and claimed that for  $p = 0.5$  ( $p \neq 0.5$ ) the model belongs to EW (KPZ) universality class [17–19]. Plischke *et al.* [17], showed that for  $p = 0.5$ , this model in  $1d$  is reversible and can be exactly solved by mapping to the kinetic Ising model. They found  $\alpha = 1/2$  and  $z = 2$ . Furthermore for  $p \neq 0.5$ , they mapped the interface model onto the driven

hard-core lattice gas, and focused on the average slope of the interface, so in an approximate way they showed that the equation of average slope is in agreement with the Burgers’s equation [17]. Thus claiming that the universality class is that of KPZ equation for  $p \neq 0.5$ . They also simulated this model for  $p = 0.0, 0.25$ , and claimed that in the limit large  $L$ , the exponent  $z$  converges to  $z_{\text{KPZ}} = 3/2$ . Simulations by the same authors on SSM in  $2d$  [18], provided the scaling exponents  $\alpha \approx 0$ ,  $z \approx 2$  for  $p = 0.5$ , and  $\alpha \approx 0.375$ ,  $z \approx 1.64$  for  $p = 0$ . Kondev *et al.* [19], simulated SSM on the square lattice with size  $L = 128$ . They confirmed that  $p = 0.5$  shows Gaussian behaviour whereas  $p = 0.1$  shows KPZ behaviour. However they found that  $p = 0.3$  consistently resembles  $p = 0.5$  contrary to claims of [17], attributing this to the above mentioned crossover from initial Gaussian behavior.

We ran large simulations in  $2d$  for SSM, and estimated interface exponents and scaling relation for the iso-height clusters and contours. Our findings are consistent with the above within numerical errors. Furthermore we checked SLE evidence for the iso-height contours and found that for  $p = 0$ , the curves are described by  $\text{SLE}_{8/3}$ . But for other values of  $p$ , the results of SLE evidence, are not compatible with each other. Our guess is that the iso-height curves can be described

by SLE, if we choose correct boundary conditions for interface. For this purpose, we have checked the SLE evidence for domain walls of critical Ising model under two different boundary conditions, and the results were consistent.

This paper is organized as follows, in section II we describe our simulations and the interface exponents, in section III we describe the ensembles of the iso-height contours, and in section IV we test for SLE curves for several values of  $p$ .

## II. INTERFACE EXPONENTS

We ran simulations on a square lattice of size  $50 \leq L \leq 700$ , averaging  $w(t, L)$  over more than 200 independent runs. Size  $L = 4000$  was used only for computing  $\beta$ . To calculate the exponents of iso-height clusters and loops, more than  $10^4$  height configurations were undertaken on square lattice with size  $L = 1000$ . Also in the part of SLE, strip geometry  $L_x = 3L_y$  and  $L_y = L$  was considered with  $100 \leq L \leq 1000$ . We define one time step as equivalent to  $L^2$  tries for deposition or evaporation.

To check the efficacy of our simulations, we calculated the roughness exponent  $\alpha$  from *scale-dependent curvature* in saturation regime. The definition of curvature  $C_b(\mathbf{x})$  at

$\mathbf{x}$  on scale  $b$ , is [19]

$$C_b(\mathbf{x}) = \sum_{m=1}^M [h(\mathbf{x} + b\mathbf{e}_m) - h(\mathbf{x})]. \quad (5)$$

The offset directions  $\{\mathbf{e}_m\}_{m=1}^M$  are a fixed set of vectors summing to zero. In our case (square lattice),  $\{\mathbf{e}_m\}$  pointing along the  $\{10\}$  type directions. For a self-affine surface, the curvature satisfies the relation [19]:

$$\langle C_b(x)^q \rangle \sim b^{\alpha_q} \quad \text{with } \alpha_q = q\alpha, \quad (6)$$

where  $\langle \cdot \rangle$  denotes spatial averaging. To check this relation, simulations were done on square lattice of size  $L = 10^3$  with more than  $10^4$  height configurations. We applied periodic boundary conditions in both directions. The results for three different values of  $q$ , are plotted in fig. 1. As expected from self-affinity, the three curves should coincide with each other, which is the case within error bars. We have excluded the point  $p = 0.5, q = 3$ , since curvature vanishes.

The interface exponents  $\alpha, \beta, z$  for various values of  $p$  are plotted in fig. 2. For  $p = 0$ , these exponents are in good agreement with the KPZ universality class [6–8]. As expected the values of  $\alpha$  and  $\beta$  decrease with  $p$ , until  $p$  reaches 0.5, where EW exponents are observed. Also near  $p = 0.5$ , we have checked that the interface exponents satisfy the logarithmic scaling relation. So far the observed behaviour at  $p = 0$  and 0.5 is in agreement

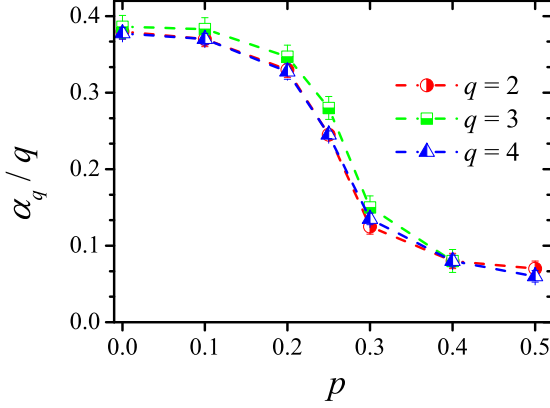


FIG. 1: Three plots correspond to  $\alpha_q/q$  versus  $p$ . As expected from self-affinity, the three curves should coincide with each other, which is the case within error bars.

with known results. Nevertheless, the behavior of these exponents in the intermediate region is unclear (see fig. 2). We observe that  $z$  increases to  $\approx 2.04$  while  $p$  is increased to 0.25. For  $p > 0.25$ , the exponent  $z$  remains constant at  $\approx 2$ . This is however not conclusive due to finite-size effects and small simulations.

### III. STATISTICS OF CLUSTERS AND LOOPS

In this section we look at the iso-height contours and clusters which can give extra information regarding self-affine interfaces [19, 21].

Consider an ensemble of height configurations in the saturated regime and look at contours at a specific height say  $h_\delta =$

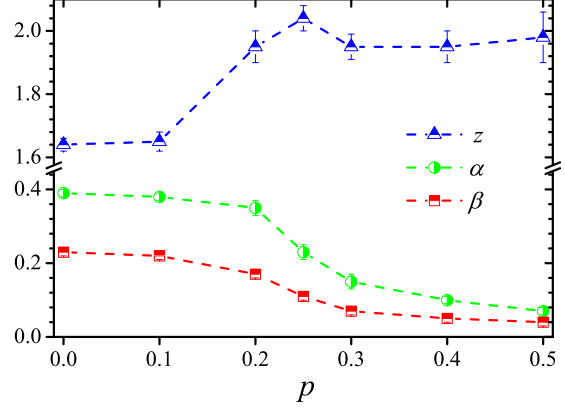


FIG. 2: (Color online) Interface exponents  $\alpha, \beta$  and  $z$  versus  $p$ . Simulations were ran on a square lattice of size  $50 \leq L \leq 700$ . Size  $L = 4000$  was used only for computing  $\beta$ .

$\langle h \rangle + \delta \sqrt{\langle [h(x) - \langle h \rangle]^2 \rangle}$ , where  $\delta$  is a small real number setting how far around the average height we are cutting the interface profile. Each island (or cluster height) is defined as a set of connected sites with positive height which identified by the Hoshen-Kopelman algorithm [22]. In this section we choose  $\delta = 0$ . The contour loops were uniquely determined by the algorithm explained in [23]. A continuous geometric change is shown in fig. 3 by snapshots of the positive height clusters for various  $p$ . The ones with lower  $p$  have much dense clusters while for higher  $p$  the clusters become more porous and scattered.

*Fractal dimensions:* One can expect (from self-similarity of clusters) a relation between the average mass of a cluster  $M$  and the radius of gyration  $R$ , i.e.,  $M \sim R^{D_c}$ , where  $D_c$  is the fractal dimension of clusters. The scal-

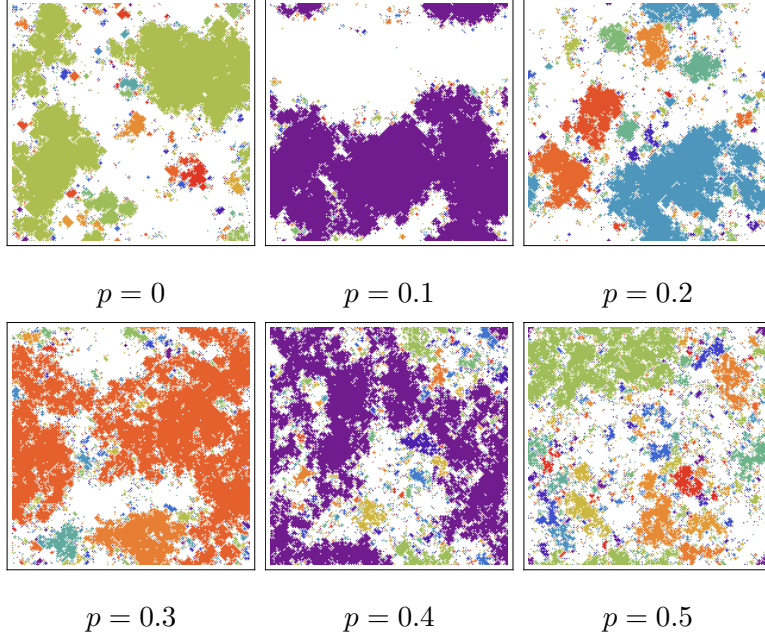


FIG. 3: (Color online) Snapshots of positive iso-height clusters for various  $p$  on a square lattice of size 200. The cut is made at the average height.

ing relation between the average length of a cluster boundary  $l$  and its radius of gyration  $r$ , is given by  $l \sim r^{d_f}$  [19, 21]. Moreover, the relation between the average area of a loop and its perimeter is  $l \sim a^{d_a}$  where  $d_a = d_f/2$  (for clusters without holes). We took more than  $10^4$  height configurations on square lattice with size  $L = 1000$  for averaging. Among them, we only present the plots of  $l(r)$  for several  $p$  in fig. 4. The corresponding exponents are reported in fig. 5. We see that the scaling exponents such as  $d_f$  and  $D_c$  for  $p = 0$  are similar to the ones for KPZ model [13, 15]. When  $p$  is increased, the value of  $d_f$  ( $D_c$ ) increases (decreases) until it approximately reaches 1.5 (1.91), in good agreement with corresponding exponents of

EW model [13, 24]. We have checked that the value of the exponents does not depend on the level of the height cut, although the range of scaling is affected after a certain distance from a critical level height [25]. In order to see the finite-size effects, we have also considered the reevaluation of the exponents by going to the lattices of larger size up to  $L = 3000$  and by taking averages over a number of 2500 saturated height configurations and obtained similar results within error bars.

*Distribution Exponents:* We now look at the distribution functions of different statistical observables of the height clusters and contours, such as the contour length distribution  $n(l)$ , cluster size distribution  $n(M)$

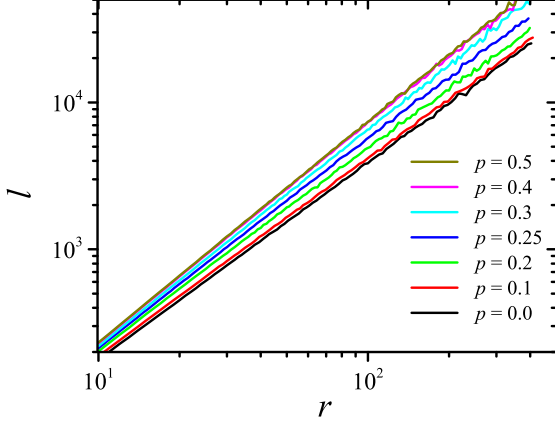


FIG. 4: (Color online) The average length of a cluster loop boundary versus the average radius of gyration on square lattice with size  $L = 1000$ . Averages are taken over more than  $10^4$  height configurations, each of them containing several iso-height clusters.

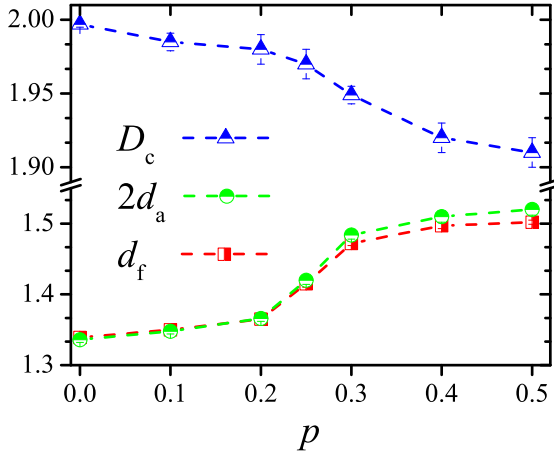


FIG. 5: (Color online) Scaling exponents of iso-height loops versus  $p$ .

and distributions for the radius of gyration of the contours and clusters, i.e.,  $n(r)$  and  $n(R)$ , respectively. These distributions are expected to follow the scaling forms,  $n(l) \sim l^{-\tau_l}$ ,  $n(M) \sim M^{-\tau_M}$ ,  $n(r) \sim r^{-\tau_r}$  and  $n(R) \sim$

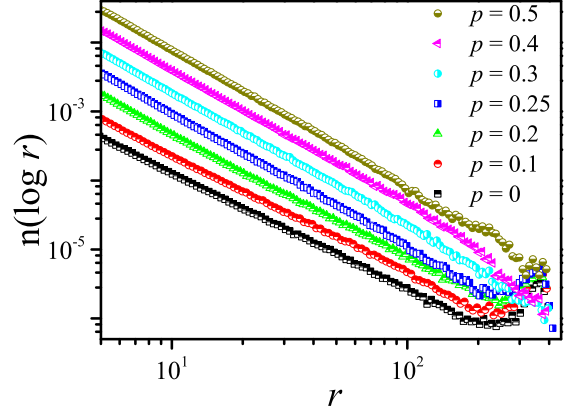


FIG. 6: (Color online) Distribution function of  $\log r$  versus  $r$  (loop's gyration radius) on square lattice of size  $L = 1000$ , for various values of  $p$ . The slope gives the exponent  $\tau_r - 1$  shown in fig. 7. For more clarity, the curves are suitably shifted.

$R^{-\tau_R}$  [19, 21]. Simulations were run on square lattice of size  $L = 1000$ , to get more than  $10^4$  height configurations for  $\delta = 0$ . The distribution function of  $\log r$  versus  $r$  is shown in fig. 6.

All distribution exponents are reported in fig 7. The dependence of these exponents on  $p$  is evident. The exponents  $\tau_R$  and  $\tau_r$  coincide within error bars. In the following, we will show that these distribution exponents depend on level cut  $\delta$ , previously noted by Olami *et al.* [26]

*Dependence of exponents on the level of the cut:* We now look at the dependence of our results on level cut  $\delta$ . All previous results were obtained at  $\delta = 0$ . We ran a number of simulations for several values of  $\delta$ , and

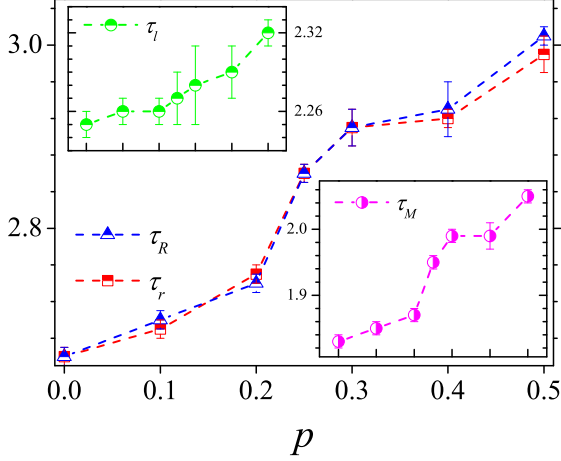


FIG. 7: (Color online) Distribution exponents (see text) versus several  $p$ .

concluded that the exponents such as fractal dimension of contours  $d_f$  and clusters  $D_c$ , do not depend on the level cut. Also we computed the exponents for the island size distributions as a function of  $\delta$ . We observe in fig. 8 that for  $p = 0.5$  and  $p = 0.3$  (and for  $p = 0.4$  as well not shown in the figure), the cluster-size exponent has a bowl-like functionality to  $\delta$ . For large  $p$ , it has a much convexity around a certain level  $\delta_{\min}$  where the exponent reaches to its minimum value. However for  $p < 0.25$ , the exponents  $\tau_M$  monotonically decreases with  $\delta$ . We have also computed  $\tau_l(\delta)$  (fig. 7) and  $\tau_r(\delta)$  (not shown), and obtained the same behaviour. Observe that error bars are larger for  $\delta < 0$ , since in this region the number of positive iso-height clusters are scarce.

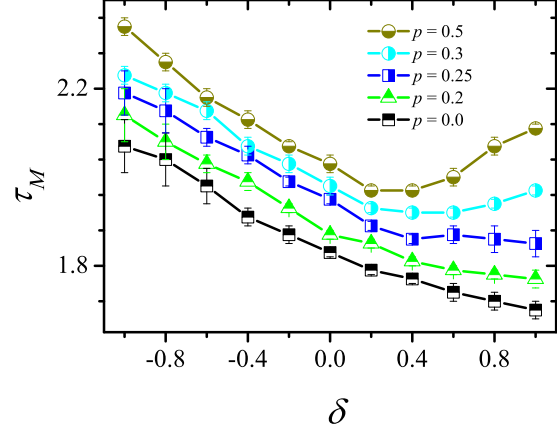


FIG. 8: (Color online) The island-size distribution exponent as a function of the level cut for various  $p$ .

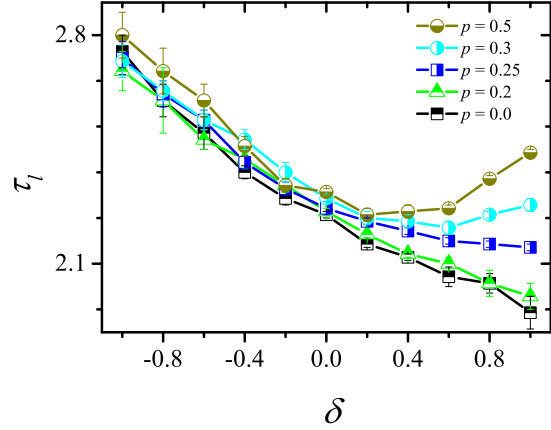


FIG. 9: (Color online) The exponent  $\tau_l$  describing the power-law behaviour of the distribution of the cluster boundary length as a function of  $\delta$ .

#### IV. EVIDENCE FOR SLE CURVES

In this section, the results are based on a series of extensive simulations of SSM on a strip geometry of size  $L_x \times L_y$  with  $L_x = 3L_y$  and  $L_y = L$ , in accord with the postulation of dipolar SLE. For each height con-



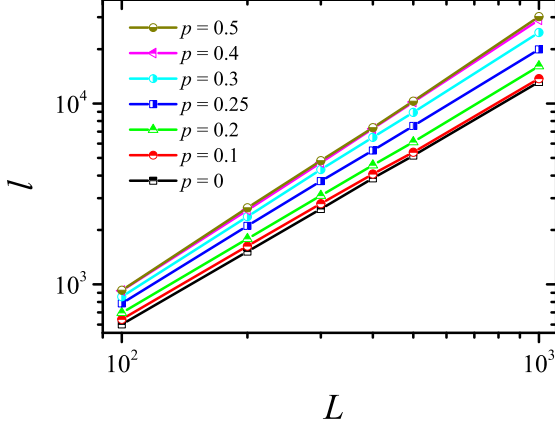


FIG. 10: (Color online) The length of spanning curves versus size of lattice  $L_y = L$ ; slope of each line (correspond to the each  $p$ ) yields  $d_f(p)$ .

figuration, we find all spanning clusters at level  $\delta = 0$  in  $y$  direction, and assign corresponding coastlines that connect the lower boundary to the upper one. We considered  $L = 100, 200, 300, 400, 500, 1000$  and examined the scaling relation  $l \sim L^{d_f}$ , in order to compute the fractal dimension of the spanning curves. We could gather a number of  $10^4$  sample curves from an approximately 7500 independent saturated height profiles. The results of the fractal dimensions for various  $p$ , are summarized in fig. 10 and the first column of table I. They show a continuous dependence of  $d_f$  on  $p$  ranging from  $4/3$  to  $3/2$  for  $p = 0$  to  $0.5$ , respectively. For conformally invariant curves, the fractal dimension is related to the diffusivity  $\kappa$  by the relation  $d_f = 1 + \kappa/8$  [9, 10, 27, 28].

To investigate if this relation holds, we com-

pute the winding angle  $\theta$  as defined by Wieland and Wilson [29]. For each curve we attribute an arbitrary winding angle to the first edge (that is set to be zero). The winding angle for the next edge is then defined as the sum of the winding angle of the present edge and the turning angle to the new edge measured in radians. The variance of the winding angle is believed to behave like  $\langle \theta^2 \rangle \sim a + b \ln L$  [29], where for conformal curves  $b = \frac{\kappa}{4} = 2(d_f - 1)$ . We have computed the variance of winding angle of an ensemble of spanning iso-height curves for different  $p$  as a function of lattice-width size  $L$ , and confirmed that is linearly proportional to its logarithm with a universal coefficient  $b$  which depends on  $p$  (see fig. 11 and table I). The two fractal dimensions obtained from direct measurement and the one derived from the coefficient  $b$ , i.e.,  $d_f = b/2 + 1$ , are plotted in fig. 12 for a comparison. They almost coincide for  $p \geq 0.25$  but with a small deviation for  $p < 0.25$ .

Let us now measure the diffusivity  $\kappa$  from a direct SLE test by statistical analysis of the driving function  $\xi_t$  of the spanning curves. For an ensemble of proposed dipolar SLE curves with hull  $K_t$ , in a strip geometry  $\mathbb{S}_\Delta = \{z \in \mathbb{C}, 0 < \Im z < \pi\Delta\}$  of width  $\pi\Delta$ , the evolution of the conformal map  $g_t(z)$  which maps

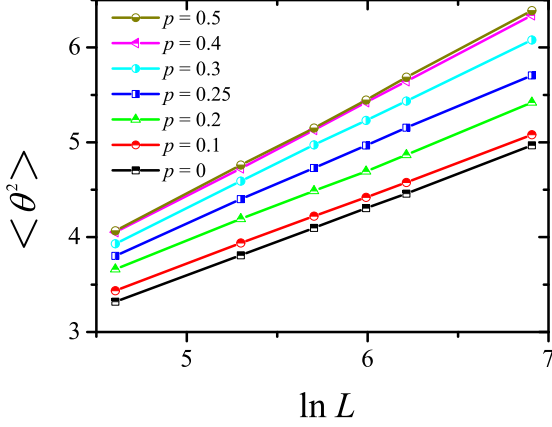


FIG. 11: (Color online) The variance of winding angle versus logarithm of the lattice width for various  $p$ .

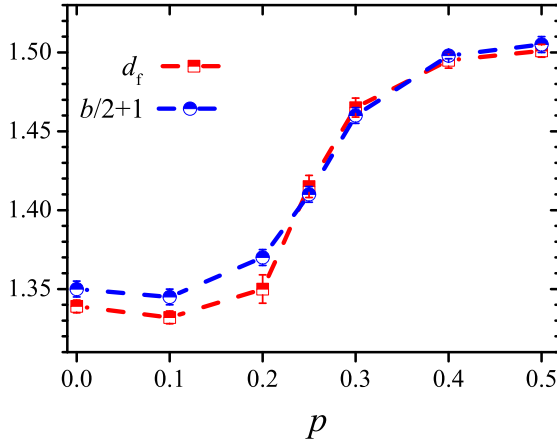


FIG. 12: (Color online) The fractal dimensions obtained from scaling relation  $l \sim L_f^d$  (squares) compared with the one derived from the slope of the linear plots in fig. 11 (circles).

$\mathbb{S}_\Delta \setminus K_t$  to  $\mathbb{S}_\Delta$  is given by [30]

$$\frac{dg_t}{dt} = \frac{1/\Delta}{\tanh((g_t(z) - \xi_t)/2\Delta)}, \quad (7)$$

with initial condition  $g_0(z) = z$ . In order to calculate sequences  $\xi(t_i)$  for the iso-height curves, we used the algorithm introduced

$p$	$d_f$	$\kappa = 8(d_f - 1)$	$b$	$\kappa = 4b$
0.00	1.339(4)	2.71(3)	0.70(1)	2.80(4)
0.10	1.332(4)	2.66(3)	0.69(1)	2.80(4)
0.20	1.350(9)	2.8(7)	0.74(1)	2.96(4)
0.25	1.415(7)	3.32(6)	0.82(1)	3.28(4)
0.30	1.465(6)	3.72(5)	0.92(1)	3.64(4)
0.40	1.495(5)	3.96(5)	0.996(4)	3.98(2)
0.50	1.501(4)	4.01(2)	1.01(1)	4.04(4)

TABLE I: First column is the fractal dimension of spanning curves  $d_f$  and second column is  $\kappa$  that is derived from  $d_f$ . The third column  $b$  is the coefficient of the variance of winding angle  $\langle \theta^2 \rangle$  plotted in fig. 11, followed by the derived values of  $\kappa$  from  $b$  in the last column.

in [31]. First we consider the sequence of the points of a spanning curve as  $z_i^0 = (x_i^0, y_i^0)$ ,  $i = 0 \cdots N$ ; the upper index represents time step, where  $t_0 = 0$  and  $\xi_0 = \xi(t_0) = 0$ . At the  $i$ th step, we map the sequence  $\{z_{i-1}^{i-1}, z_i^{i-1}, \dots, z_N^{i-1}\}$  to the transformed and shortened sequence  $\{z_i^i, z_{i+1}^i, \dots, z_N^i\}$ , by using the map appropriate for dipolar SLE,

$$t_i = t_{i-1} - 2(L/\pi)^2 \log [\cos(\Delta_i)], \quad (8)$$

$$z_j^i = \xi_i + \frac{2L}{\pi} \cosh^{-1} \left\{ \frac{\cosh[\pi(z_j^{i-1} - \xi_i)/2L]}{\cos \Delta_i} \right\},$$

where  $\Delta_i = \pi y_i^{i-1}/2L$  and  $\xi_i = x_i^{i-1}$ . For SLE curves, the driving function satisfies  $\xi(t) = \sqrt{\kappa} B_t$  [10, 30], where  $B_t$  is the Brownian motion.

Another test of conformal invariance, is to compute the *left passage probability*  $P(\rho, \phi)$ , defined as the probability that a curve in the upper half-plane, passes to the left of a given point at polar coordinates  $(\rho, \phi)$ . This is given by Schramm's formula [32]:

$$P_k(\phi) = \frac{1}{2} + \frac{\Gamma(\frac{4}{\kappa})}{\sqrt{\pi}\Gamma(\frac{8-\kappa}{2\kappa})} \cot(\phi) \times {}_2F_1\left(\frac{1}{2}, \frac{4}{\kappa}; \frac{3}{2}; -\cot^2(\phi)\right), \quad (9)$$

where  ${}_2F_1$  is the hypergeometric function. Although this equation is originally obtained for chordal SLE curves, it also holds for dipolar SLE with  $\rho \ll L$  [31].

We considered a substrate of strip geometry with size  $L_x/3 = L_y = L = 1000$ , and extracted all spanning contour lines at the level  $\delta = 0$ , with total number of  $10^4$ . We then extracted the underlying driving function for each value of  $p = 0, 0.1, 0.2, 0.25, 0.3, 0.4, 0.5$  and examined if the result is in accord with the postulates of conformal invariance and that of predicted by Schramm's formula. We found that (see fig. 13) for  $p = 0$ , the diffusivity derived from driving function is  $\kappa = 2.56(6)$  and from left-passage  $\kappa = 2.55(8)$  which is approximately compatible with fractal dimension of curves reported in table I. This is very close to the diffusivity of self-avoiding walk (SAW) with  $\kappa = 8/3$  [33, 34]. But for other values of  $p$ , we saw that the diffusivity derived from left-passage and driving function  $\xi(t)$  is incompatible with our

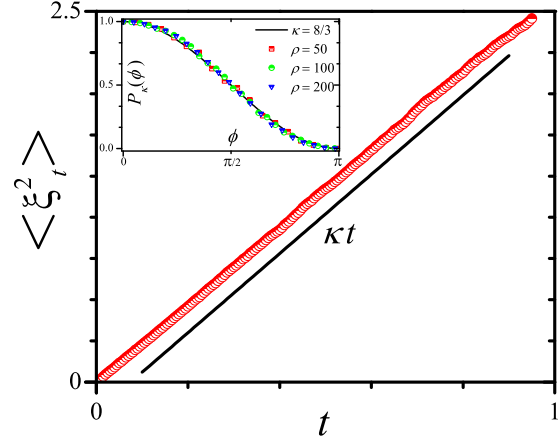


FIG. 13: (Color online) Main: the variance of driving function versus time (which is normalized to 1). The slope of line gives  $\kappa \approx 8/3$ . Inset: the left-passage probability versus polar coordinate  $\phi$ . The solid curve is the exact value of  $P_{\kappa=8/3}(\phi)$ , and the three plots correspond to different radii. These results are for  $p = 0$ .

previous results in table I. For instance, for  $p = 0.5$ , we obtain  $\kappa \approx 2.24(5)$ , which is clearly different from  $\kappa_{EW} = 4$  [24].

Our guess is that the statistics of the spanning curves are affected by the imposed boundary conditions in our simulations. To see how this can affect our results, we considered critical Ising model on a strip geometry ( $L_x/4 = L_y$ ) with two different boundary conditions:

- (i) Fixed boundary condition, i.e., all spins in the right and left sides of the origin (located at the middle of the lower boundary on  $x$  axis) are fixed to be up and down,

respectively. Anti-periodic BC was applied along the  $x$  direction and the spins at the upper boundary were left free. Such BCs imposes the interface (domain wall that separate spins up from down) emanating from the origin to go towards the upper boundary. We checked that the spanning interfaces are well described by the prediction of SLE with  $k \approx 3$  and  $d_f \approx 11/8$  [35, 36].

(ii) Free boundary conditions along both directions. In this case, the fractal dimension of these curves is  $d_f \approx 11/8$ , but the diffusivity that is derived from left-passage probability and the driving function is  $\kappa \approx 2$ . These results show that all critical interfaces don't satisfy the SLE relation.

We also simulated critical percolation

model on a strip geometry with the same two boundary conditions. We found the diffusivity  $\kappa \approx 6$  [37] compatible with fractal dimension  $d_f \approx 7/4$  [38], for both BCs. This result is expected since for the percolation model, the statistics of the domain walls are not affected by the BCs due to a locality property [10, 28].

In SSM, only for  $p = 0$ , we obtain the compatibility between fractal dimension and diffusivity that is in SAW universality class. It is known that the outer perimeter of critical percolation clusters in  $2d$  are described by SAW [39]. In our recent work [12], we have shown that the iso-height lines of various discrete models including BD, RSOS and EDEN models are in the SAW universality class.

- 
- [1] A. Barabási and H. Stanley, *Fractal concepts in surface growth* (Cambridge university press, 1995).
  - [2] P. Meakin, *Fractals, scaling and growth far from equilibrium*, Vol. 5 (Cambridge university press, 1997).
  - [3] F. Family and T. Vicsek, Journal of Physics A: Mathematical and General **18**, L75 (1985).
  - [4] S. F. Edwards and D. R. Wilkinson, Proceedings of the Royal Society of London. A. Mathematical and Physical Sciences **381**, 17 (1982).
  - [5] M. Kardar, G. Parisi, and Y. C. Zhang, Physical Review Letters **56**, 889 (1986).
  - [6] J. G. Amar and F. Family, Physical Review A **41**, 3399 (1990).
  - [7] E. Marinari, A. Pagnani, and G. Parisi, Journal of Physics A: Mathematical and General **33**, 8181 (2000).
  - [8] V. G. Miranda and F. D. A. A. Reis, Physical Review E **77**, 031134 (2008).
  - [9] O. Schramm, Israel Journal of Mathematics **118**, 221 (2000).

- [10] M. Bauer and D. Bernard, Physics reports **432**, 115 (2006).
- [11] K. Löwner, Mathematische Annalen **89**, 103 (1923).
- [12] A. A. Saberi, H. Dashti-Naserabadi, and S. Rouhani, Physical Review E **82**, 020101 (2010).
- [13] A. A. Saberi, M. D. Nir, S. M. Fazeli, M. R. R. Tabar, and S. Rouhani, Physical Review E **77**, 051607 (2008).
- [14] A. A. Saberi, M. A. Rajabpour, and S. Rouhani, Physical review letters **100**, 44504 (2008).
- [15] A. A. Saberi and S. Rouhani, Physical Review E **79**, 036102 (2009).
- [16] P. Meakin, P. Ramanlal, L. M. Sander, and R. C. Ball, Physical Review A **34**, 5091 (1986).
- [17] M. Plischke, Z. Rácz, and D. Liu, Physical Review B **35**, 3485 (1987).
- [18] D. Liu and M. Plischke, Physical Review B **38**, 4781 (1988).
- [19] J. Kondev, C. L. Henley, and D. G. Salinas, Physical Review E **61**, 104 (2000), arXiv:9907229v1 [cond-mat].
- [20] J. M. Kim and J. M. Kosterlitz, Physical review letters **62**, 2289 (1989).
- [21] J. Kondev and C. L. Henley, Physical review letters **74**, 4580 (1995).
- [22] J. Hoshen and R. Kopelman, Physical Review B **14**, 3438 (1976).
- [23] A. A. Saberi, Journal of Statistical Mechanics: Theory and Experiment **2009**, P07030 (2009).
- [24] O. Schramm and S. Sheffield, Probability Theory and Related Fields , 1 (2010).
- [25] A. A. Saberi, Applied Physics Letters **97**, 154102 (2010).
- [26] Z. Olami and R. Zeitak, Physical review letters **76**, 247 (1996).
- [27] J. Cardy, Annals of Physics **318**, 81 (2005).
- [28] I. A. Gruzberg, Journal of Physics A: Mathematical and General **39**, 12601 (2006).
- [29] B. Wieland and D. B. Wilson, Physical Review E **68**, 056101 (2003).
- [30] M. Bauer, D. Bernard, and J. Houdayer, Journal of Statistical Mechanics: Theory and Experiment **2005**, P03001 (2005).
- [31] D. Bernard, P. Le Doussal, and A. A. Middleton, Physical Review B **76**, 020403 (2007).
- [32] O. Schramm, Electron. Comm. Probab **6**, 115 (2001).
- [33] T. Kennedy, Physical review letters **88**, 130601 (2002).
- [34] G. F. Lawler, O. Schramm, and W. Werner, (2002), arXiv:math/0204277v2 [math.PR].
- [35] S. Smirnov, (2007), arXiv:0708.0039 [math-ph].
- [36] A. Gamsa and J. Cardy, Journal of Statistical Mechanics: Theory and Experiment

- 2007**, P08020 (2007). view letters **58**, 2325 (1987).
- [37] S. Smirnov, Comptes Rendus de l'Académie des Sciences-Series I-Mathematics **333**, 239 (2001). [39] V. Beffara, Annals of probability , 2606 (2004).
- [38] H. Saleur and B. Duplantier, Physical re-